Progress In Electromagnetics Research C, Vol. 94, 273–283, 2019

Design and Characterization of a Broadband Flexible Polyimide RFID Tag Sensor for NaCl and Sugar Detection

Mohammed A. Ennasar[1], Otman El Mrabet[2, *], Kanjaa Mohamed[2], and Mohamed Essaaidi[1, 2]

Abstract—In this paper, we present a broadband flexible RFID sensor tag antenna to detect the concentration of aqueous solutions. The proposed RFID tag antenna sensor with a T matching network is based on a printed dipole whose arms are loaded with circular disk patches. The structure is printed on a Kapton polyimide flexible substrate. The sensing mechanism of the RFID tag antenna is based on the change of sensitivity of the RFID tag antenna that occurs with the variation of aqueous solution concentration. The proposed sensor is designed using CST Microwave studio, and its various parameters are optimized in order to have a broadband impedance matching that covers the entire RFID band (860–960 MHz). The experimental setup is small, rapid, contactless, and inexpensive. Results are presented for NaCl and sugar aqueous solutions with concentrations ranging from 0% to 80%.

1. INTRODUCTION

The widespread use of sugar and NaCl in many consumer products especially in food and beverages industry may increase the risk of obesity, diabetes, high blood pressure, heart disease, stroke, and kidney problems [1–3]. Thus, the accurate measurement of sugar and NaCl concentrations is of great interest. Up to now, several techniques have been proposed to measure the concentration of liquid solutions and especially sugar and NaCl concentrations. Recently, RF and microwave sensors have gained much attention owing to their numerous advantages compared to traditional techniques. For example, in [4], the authors developed a microstrip antenna-based sensor for detecting NaCl and sugar contents in water. Gennarelli et al. [5] proposed a waveguide cavity-based sensor for measuring the concentration of liquid solutions, and Albishi and Ramahi [6] introduced a new concept based on increasing capacitance that interacts with the liquid under test to increase the sensitivity of planar electrically resonators when being used as near field sensors. Most of these techniques require expensive instruments such as network analyzer and are operator dependent (many training sessions needed for not specialized persons). In addition to their higher cost and complexity, all these approaches are time consuming and require a direct contact with the liquid. Therefore, there is a clear need to develop new techniques which are low cost, rapid, contactless, and suitable to be used in lab on chip.

Recently, there has been increasing interest in developing tag antenna-based sensors using Radio Frequency Identification (RFID) owing to their passive, wireless, and low-cost characteristics [7]. Due to the aforementioned reasons, many RFID tag antennas-based sensing has been proposed in literature [8–16]. These works extend the field of application of this technology that until now has been limited to tracking information and identifying objects in different supply chains. In this paper, we address the challenge of measuring the concentration of sucrose and NaCl in liquid solutions using UHF-RFID technology. Thus, an RFID tag antenna printed on a flexible substrate operating at the UHF band

Received 24 May 2019, Accepted 23 July 2019, Scheduled 6 August 2019

* Corresponding author: Otman El Mrabet (o.elmrabet@ac.uae.ma).

[1] Smart Systems Laboratory (SSL), Higher School of IT (ENSIAS), Mohamed V University, Rabat, Morocco. [2] Information and Telecommunication Systems Lab, Faculty of Sciences, University of Abdelmalek Essaadi, Tetouan, Morocco.

(860–960 MHz) with a dimension of $100 \times 32\,\mathrm{mm}^2$ is designed, fabricated, and mounted on a glass beaker to work as a sensor by measuring the received power (Sensitivity). The sensing mechanism is based on the change in the characteristics of the space surrounding the RFID tag. In this study, we show that the change in the conductivity and permittivity of the resulting water when adding NaCl or Sucrose affects the performance of the RFID tag. The received power has been measured by using a home-made RFID kit that includes Thing Magic Micro (M6e-M). The findings exhibit a substantial step toward a low cost, real time, and contactless monitoring system.

2. OPERATING PRINCIPLE OF RFID TAG ANTENNA AS SENSOR AND WORKING PRINCIPLE

The working principle of the proposed sensor is based on the use of the RFID technology. In this technique, the liquid under test is introduced into a glass beaker filled with liquid solution (Sucrose or NaCl) on which we paste an RFID tag antenna. The beaker is then placed near the RFID reader to ensure a backscatter communication.

In general, the sensitivity of the RFID-UHF tag antenna can be written as:

$$S_{\mathrm{tag}} = P_{tx,ON} \cdot G_{tx} \cdot \tau \cdot \left(\frac{\lambda}{4\pi d}\right)^2 \cdot \eta_{plf} \cdot A_{\mathrm{cable}} \tag{1}$$

where G_{tx} is the gain of the reader, η_{plf} the polarization mismatch, τ the transmission coefficient of the RFID tag, and A_{cable} the attenuation of the cable.

Depending on the matching between the antenna and the chip, only a fraction of this power is transferred to the latter and given by [17]:

$$S_{\mathrm{chip}} = \left(1 - |\Gamma_{\mathrm{tag}}|^2\right) \cdot G_{\mathrm{tag}} \cdot S_{\mathrm{tag}} \tag{2}$$

All the irrelevant parameters excluded and from Eqs. (1) and (2) we obtain:

$$S_{\mathrm{tag}} \alpha \frac{1}{\left(1 - |\Gamma_{\mathrm{tag}}|^2\right) \cdot G_{\mathrm{tag}}} \tag{3}$$

Since the reflection coefficient is dependent on the dielectric characteristics of the surrounding medium, any change in the latter will affect the sensitivity, hence the underlying measurement principle. The dielectric dependence on the permittivity of the sucrose and sodium chloride solutions concentration has been established respectively by Buchner et al. [18] and Malmberg and Maryott in [19] for the working frequency and for $T = 298\,\mathrm{K}$ through the fitting equations:

$$\varepsilon_{\mathrm{NaCl}}(c) = 78.45 - 15.45c - 3.76c^{3/2} \tag{4}$$

$$\varepsilon_{\mathrm{Succ}}(c) = \varepsilon_w - 0.226c - 6.75(10^{-4})c^2 - 1.09c^3 \tag{5}$$

where c is the weight percent, and ε_w is the permittivity of the pure water.

Figure 1 shows that as c increases, the static permittivity decreases changing the RFID-tag reflection coefficient Γ_{tag} and G_{tag}, and this change can be measured through S tag, which explains the underlying sensing mechanism of the RFID tag antenna.

3. RFID TAG ANTENNA: ANALYSIS AND DESIGN

The main part of the proposed sensor structure is an RFID tag antenna whose configuration is shown in Figure 2. The proposed tag antenna is of a simple design. It is based on a printed dipole whose arms are loaded with circular disk patches with a T matching network. The proposed design is printed on a $127\,\mu m$ (Kapton) polyimide flexible substrate, with a dielectric constant of 3.5 and loss tangent of 0.002. The top antenna trace is made of copper having a thickness of $35\,\mu\mathrm{m}$. The overall size of the substrate is $100 \times 32\,\mathrm{mm}^2$.

The proposed RFID tag antenna is designed to operate in the RFID-UHF band of 860–960 MHz. It covers the whole global UHF RFID frequency band. The Murata LXMS31ACNA chip with an

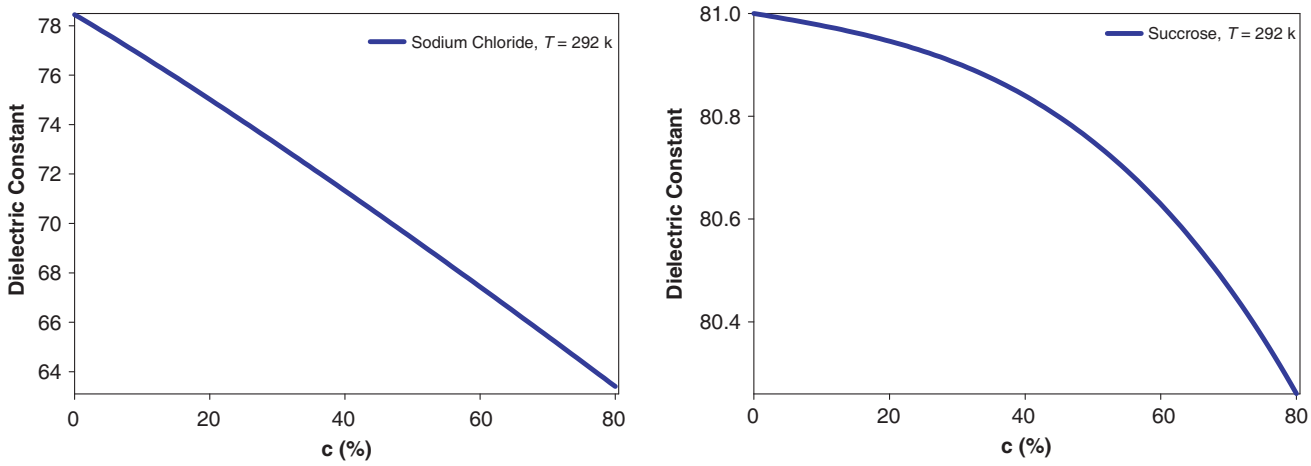

Figure 1. Concentration dependence of the dielectric constant of NaCl electrolyte solution and sucrose solution at $T = 298.15\,\mathrm{K}$ from the measurements of Buchner et al. [18] (Eq. (1)) and CG Malmberg et al. [19] (Eq. (2)).

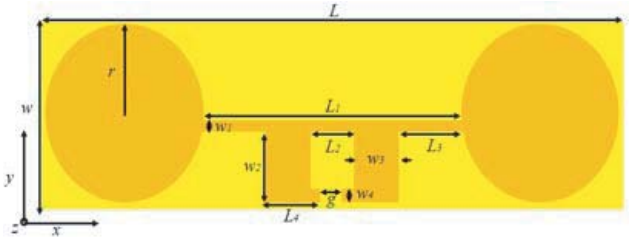

Figure 2. The geometry of the proposed RFID tag antenna.

Figure 3. Prototype of the proposed flexible tag antenna.

Table 1. Dimensions of RFID tag antenna [mm].

L	L_1	L_2	L_3	L_4	w	w_1	w_2	w_3	w_4	g	r
100	36	6	10.14	7	32	1.25	12.4	4.8	2	2	15.5

impedance of $Z_{\mathrm{Chip}} = (17.6 - j100.9)\,\Omega$ at 915 MHz is selected for our design. The minimum threshold power to activate this chip is $-8\,\mathrm{dBm}$ [20]. Note that the impedance of the chip is measured using the same method reported in [21]. Therefore, the input impedance of the antenna has to be $17.6 + j100.9\,\Omega$ so that a maximum power transfer can be achieved. The optimized geometrical parameters obtained by using CST Microwave studio are listed in Table 1.

To demonstrate the operating principle of the reactive matching of the proposed design, we propose the equivalent electrical model shown in Figure 4. For the sake of simplicity, the RFID chip and the antenna are modelled as a series RC $(R_{\mathrm{chip}}, C_{\mathrm{chip}})$ and a series RLC circuit $(R_{ant}, L_{ant}, C_{ant})$, respectively. The radiation resistance for a small dipole can be approximated by [22]:

$$R_a = 80\pi^2\alpha^2\left(\frac{l}{\lambda}\right) \tag{6}$$

where $0.5 \leq \alpha \leq 1$ depending on how the current is distributed along the antenna, and l is the length of the antenna. By considering the working frequency of the dipole antenna without T-matching at approximately 1.1 GHz, the radiation resistance is $43.39\,\Omega$ when α is equal to 0.7, and the length of the antenna is 93 mm. The inductance of the antenna is found to be 35.43 nH by using the following

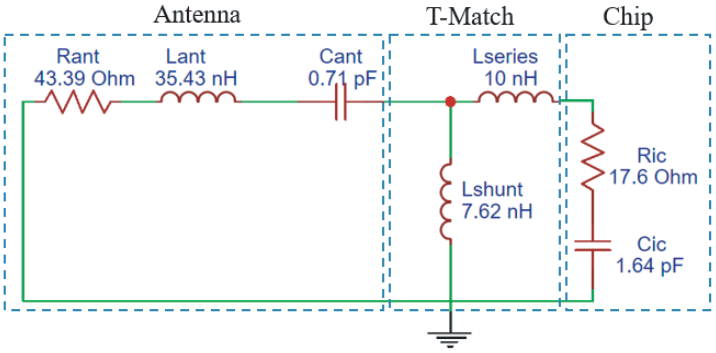

Figure 4. Equivalent circuit analysis of the antenna tag.

approximated formula given in [23]:

$$L_{ant} = \frac{\mu_0}{2\pi} l \left(\ln\left(\frac{l}{w}\right) + \frac{\pi}{2} \right); \quad \mu_0 = 4\pi \times 10^{-7}\,\mathrm{H/m} \tag{7}$$

where l and w are respectively the length and width of the conductive strip. Next, the antenna capacitance C_{ant} is found to be 0.71 pF by using Equations (8) and (9) given below. By using the self-resonant frequency of the proposed antenna where L_{ant} and C_{ant} are the equivalent inductance and capacitance, respectively, of the proposed antenna. Therefore, the capacitance C_{ant} is found to be:

$$f_c = 1/2\pi\sqrt{L_a C_a} \tag{8}$$

$$C_{ant} \approx 1/4\pi^2 f_c^2 L_{ant} \tag{9}$$

where f_c, L_{ant}, and C_{ant} are respectively the self-resonant frequency, the equivalent inductance, and the capacitance of the proposed antenna.

The equivalent circuit for MURATA RFID chip is a 17.6 Ω resistor in series with a 1.64 pF capacitor. The T-matching network can be modelled as a series inductance (L_{series}) and (C_{Shunt}).

With the lumped component values given above, the reflection coefficient S_{11} (dB) of the RFID tag antenna in free space can be obtained by using a circuit simulator (Agilent's Advanced Design System). The obtained results are plotted in Figure 5 along with S_{11} (dB) from the CST Microwave studio for ease of comparison.

Small discrepancy between full wave simulation and the equivalent circuit model can be observed. This can be ascribed to the use of the approximated equations to calculate all the lumped elements,

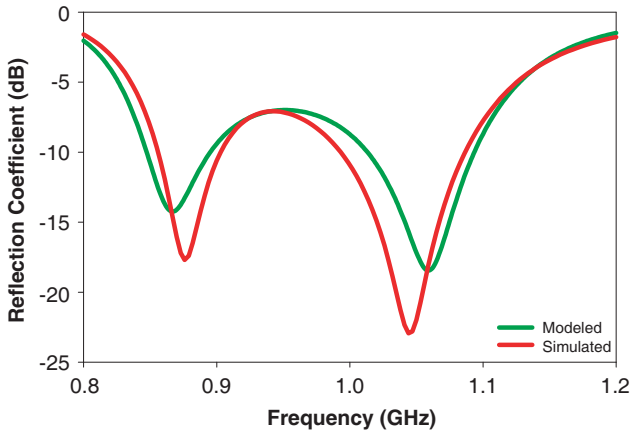

Figure 5. Comparison results between full wave simulation and the equivalent circuit model.

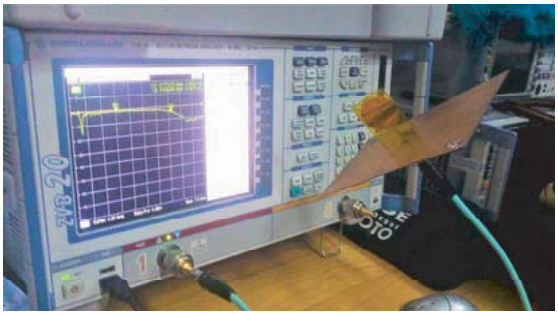

Figure 6. Measurement set-up using Rohde & Schwarz ZVB 20 VNA.

and even so, the proposed model can accurately predict the reflection coefficient. Furthermore, Figure 5 shows that the simulated −3 dB bandwidth ranges from 820 MHz to 960 MHz for a total bandwidth of 140 MHz which can totally cover the UHF-RFID band.

4. MEASUREMENTS RESULTS AND DISCUSSION

A prototype of the proposed flexible RFID (Fig. 3) tag antenna has been fabricated and tested to verify the above results. Note that the prototype shown in Figure 2 is fabricated using the following process which can be divided into different steps. First, the proposed antenna is fabricated on a thin adhesion layer as a mask by using board laser cutting machine 1390 triumph [24], then the mask is pasted on a thin sheet copper layer. The removal of the copper in the unwanted region is done by a Cu etchant to get the designed top layer of the proposed antenna. The latter, is cleaned by isopropyl alcohol and deionized water rinse and then directly attached to the Kapton polyimide flexible substrate.

The measured input impedance of the proposed design obtained using the same method reported in [25] is plotted in Figure 7. The input impedance is measured using a Rohde & Schwarz ZVB 20 Network analyzer and the image theory principle [26] as shown in Figure 6.

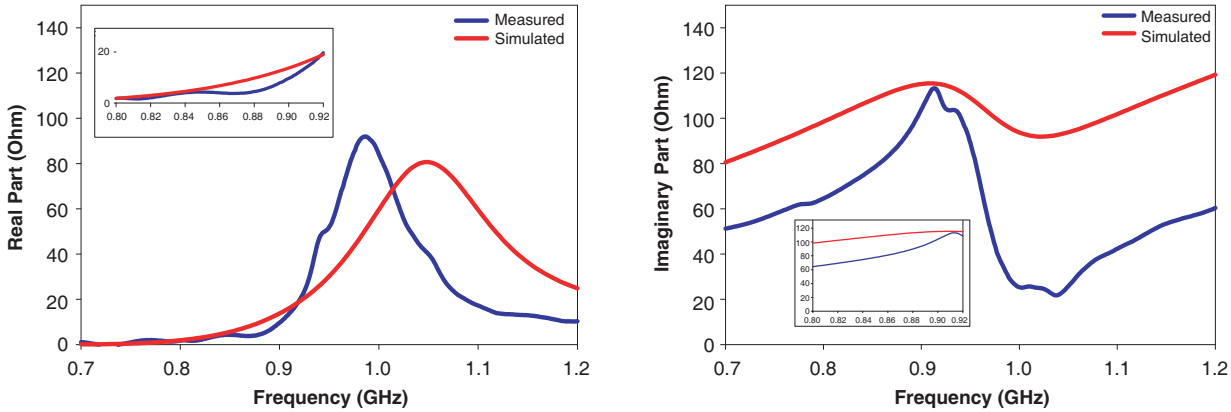

Figure 7. Input impedances of the prototype in free space. (a) Real part; (b) imaginary part.

The measured and simulated input impedances of the proposed RFID tag antenna in free space are plotted in Figure 7. From the measurement results the impedance of the antenna is approximately $(16.43 + j112.3\,\Omega)$ at 915 MHz, which is good enough to guarantee a maximum power transfer between the Murata chip $(17.6 - j100\,\Omega)$ and the antenna at this frequency.

Figure 8 shows the reflection coefficient generated from the equivalent circuit model, CST microwave studio simulation, and image theory measurement. Good agreement can be observed between the three sets of data. The measured −3 dB bandwidth ranges from 830 MHz to 1.1 GHz for a total bandwidth of 18 MHz which can totally cover the UHF RFID band.

Another more practical feature of the RFID tag antenna is the read range. This important characteristic can be calculated using the Friis equation [27]:

$$S_{\text{tag}} = P_{tx,ON} \cdot G_{tx} \cdot \tau \cdot \left(\frac{\lambda}{4\pi d}\right)^2 \cdot \eta_{plf} \cdot A_{\text{cable}} \tag{10}$$

$d_{\max}$ can be expressed as follows:

$$d_{\max} = \frac{\lambda}{4\pi}\sqrt{\frac{P_{tx,ON} \cdot G_{tx} \cdot \eta_{plf} \cdot A_{\text{cable}}}{S_{\text{tag}}(f)}} \tag{11}$$

where $P_{tx,ON}$ is the the power transmitted from the reader, G_{tx} the gain of the reader, η_{plf} the polarization mismatch, τ the transmission coefficient of the RFID tag, and A_{cable} the attenuation of the cable.

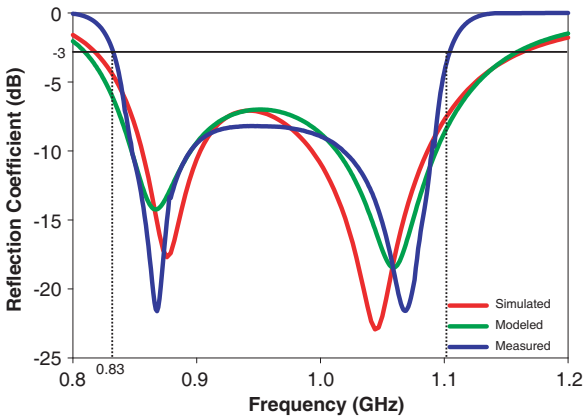

Figure 8. Simulated and measured reflection coefficient of the proposed RFID tag antenna.

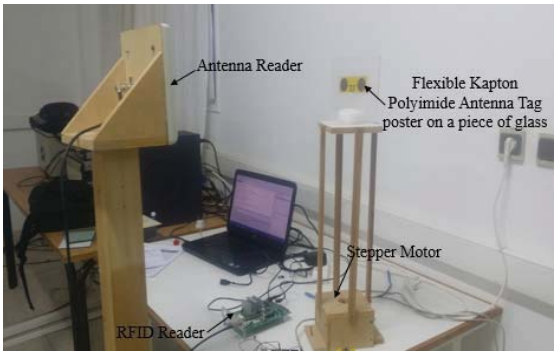

Figure 9. Measured setup read range of the proposed RFID tag antenna in ordinary room.

The measurement setup has been deployed in an ordinary room to measure the maximum read range. This measurement setup used here is similar to the one reported in [28]. It consists of a Thing Magic Micro (M6e-M) reader connected to a single circularly polarized patch antenna having a gain of 6 dBi at the frequency range of 800–1000 MHz. The RFID reader is connected to the polarized patch antenna via 1.8 m of 50 coaxial cable model CNT-195-FR to generate 36 dBm at 915 MHz. Hence, the total transmitted power is approximately 4 W EIRP (effective isotropic radiated power).

The whole system is controlled by a homemade software installed in a computer to plot the measured activation power and read range. The distance between the polarized patch antenna and RFID tag antenna in this setup, which are aligned in parallel, is 1 m to meet far field requirement.

Figure 9 represents the measured setup of the read range when the RFID tag antenna is placed on a glass piece of dimension $20 \times 20\,\text{mm}^2$. We have also measured this parameter in free space. The obtained results for the latter case (Figure 10(a)) show that the RFID tag antenna has a read range more than 4.8 m across the whole band allowed for RFID technology (860–960 MHz), and an activation power of -7.5 dBm is achieved near 915 MHz. However, when the tag is placed on a glass piece, the read range decreases, and the activation power increases as shown in Figure 10(b). This discrepancy between the two cases can be ascribed to the change in the characteristics of the space surrounding the tag when adding the glass layer, which is consistent with Equation (1). It is worthwhile to mention that the proposed structure can demonstrate farther read ranges on different objects because the RFID chip used in this paper has $P_{th} = -8$ dBm, and this value is certainly very high compared to other RFID chips like NXP G2XL and Alien Higgs. For example, if an NXP G2XL IC chip with $P_{th} = -17$ dBm is used in the design of this RFID tag antenna, the calculated read range would be more than 12 m in free space.

We have also measured the read range patterns in free space of the proposed design for the two planes at 868 and 915 MHz, respectively. The obtained results are plotted in Figure 11. We can see that the read range pattern is similar for both frequencies. In the (y-z) plane (Horizontal position), a maximum read range of 8 m in the 30° direction at 915 MHz and 7.5 m at 868 MHz is measured, as can be seen clearly from Figure 9. In (x-y) plane (Vertical position), a maximum read range of 7.5 m at 915 MHz and 7 m at 868 MHz, with a good unidirectional read range pattern, is obtained.

Next, we have measured the read range patterns when the RFID tag antenna is placed on a glass beaker for the two planes at 868 and 915 MHz, respectively (see the inset of Figure 12). It is found that the read range has been decreased which is consistence with Equation (3). Figure 12 also reveals that there is always a communication between the reader and the tag.

5. SENSOR TAG APPLICATION AND DISCUSSION

In this part, we will use the RFID tag antenna studied numerically and experimentally in the previous paragraph as a sensor to detect both ionic (sodium Chloride) and nonionic (sucrose) concentrations.

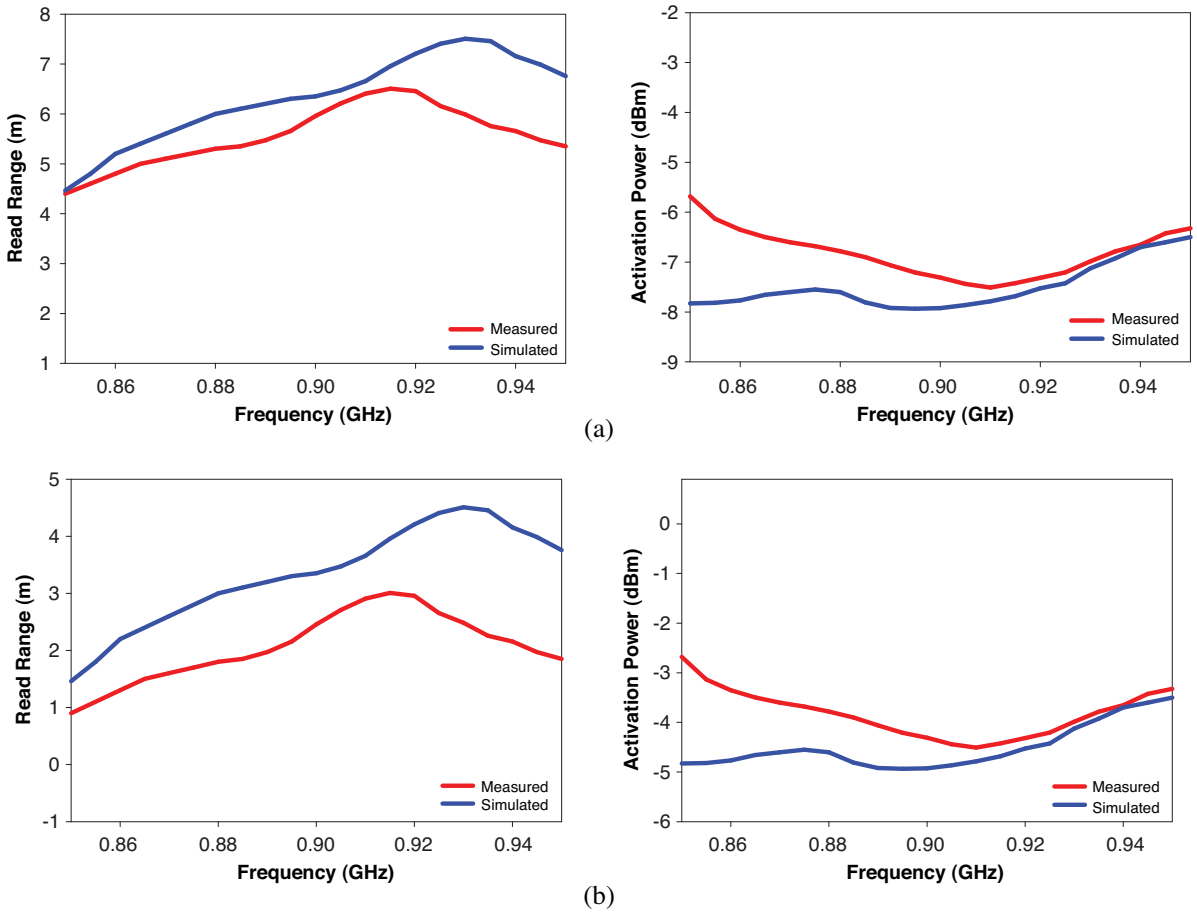

Figure 10. Read range and activation power of the proposed RFID tag antenna as a function of frequency: (a) in free space and (b) on a piece of glass.

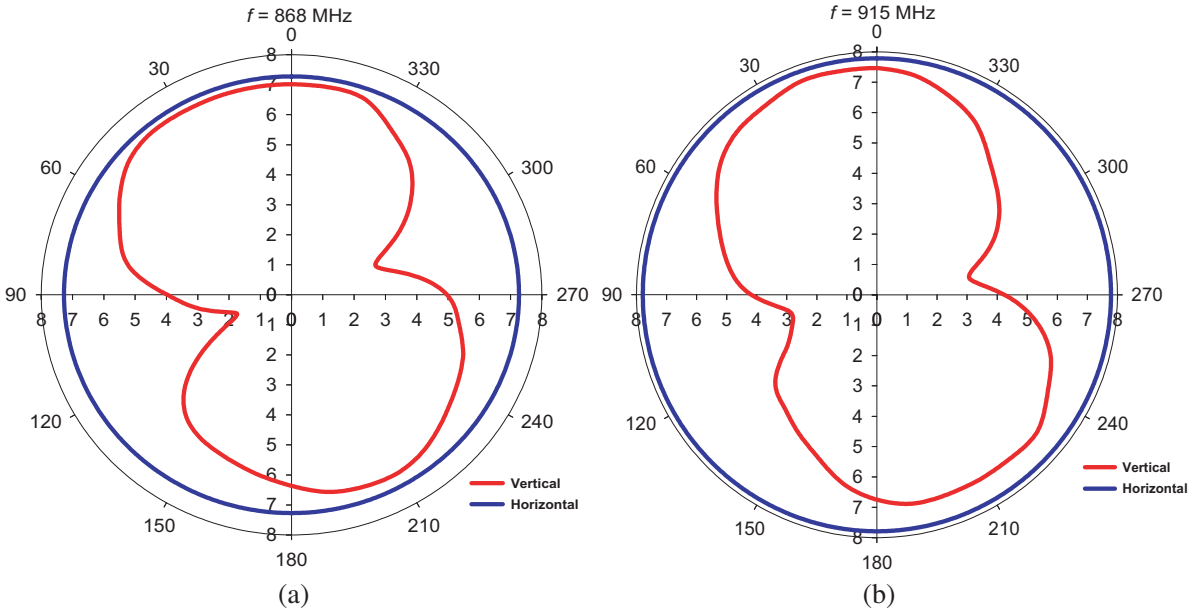

Figure 11. Measured read range patterns of the proposed RFID tag: (a) 868 MHz, (b) 915 MHz in free space.

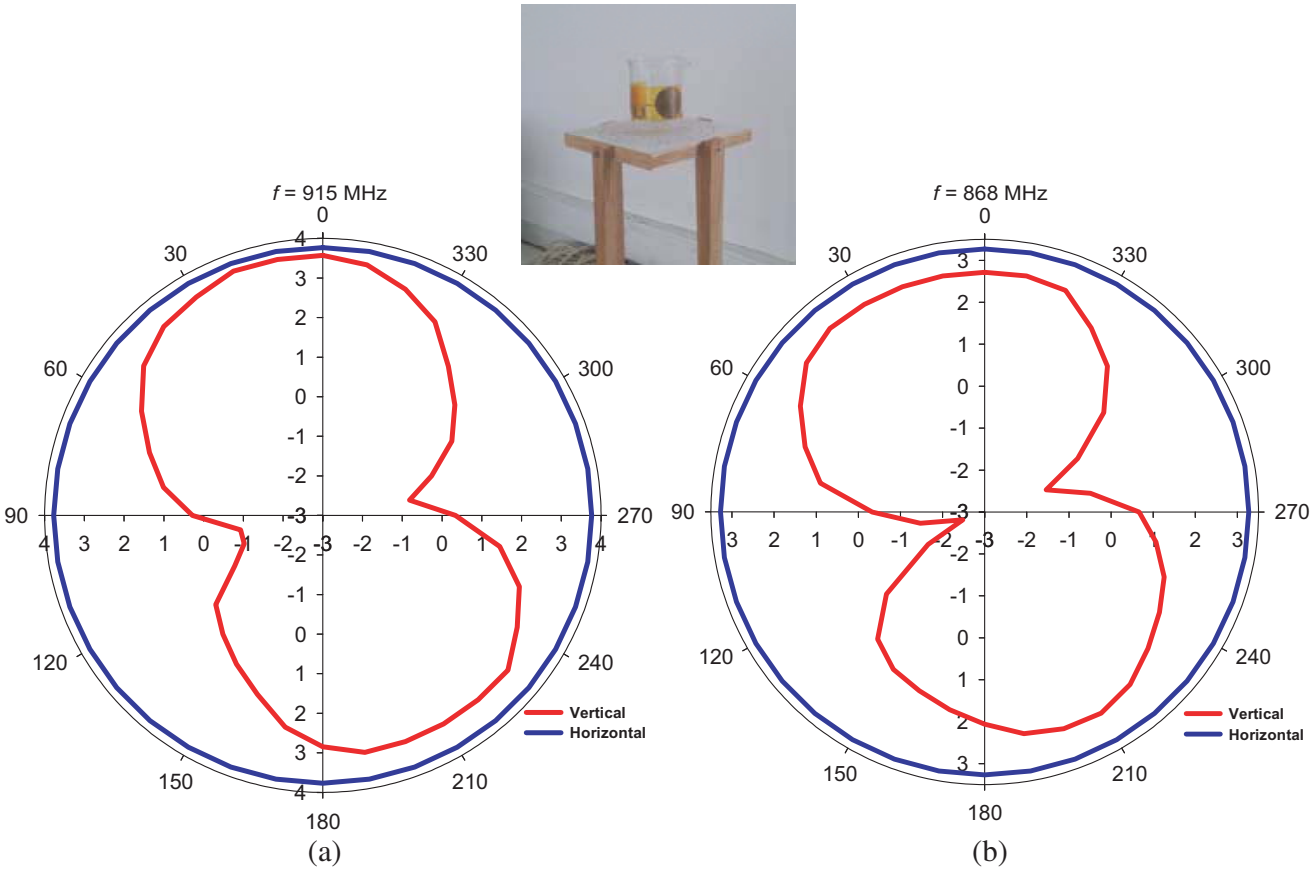

Figure 12. Measured read range patterns of the proposed RFID tag placed on empty glass beaker: (a) 915 MHz, (b) 868 MHz.

The experimental setup used in this work to measure the concentration of both aqueous solutions is depicted in Figure 13. It consists of an RFID reader, a glass beaker filled with the liquid solution under test, on which we paste an RFID tag antenna. The RFID Reader and RFID tag antenna are positioned in line of sight disposition and 0.3 m away from each other.

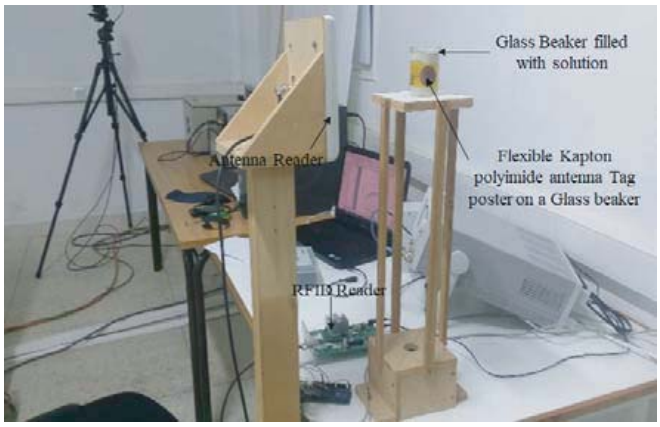

Figure 13. Photograph of the experimental set-up for the measurements of the concentration of aqueous solutions.

For validation purposes, we have prepared two aqueous solutions separately. The first one is made of distilled water and sodium chloride (NaCl). The second solution investigated in this work is made of distilled water and sucrose (C12H22O11). For the experiment, NaCl and sucrose are dissolved individually in water to prepare concentrations ranging from 0 to 80% with a step of 20%. For each concentration, the sensitivity of the RFID tag antenna is measured by stepped increasing Ptx until successfully reading the RFID tag. It is worthwhile to mention that all the measurements are performed in an ordinary room equipped with an air conditioner temperature that has been set to 20 degrees Celsius.

From Figure 14 and Figure 15 one can see that the sensitivity of the RFID tag antenna increases with the increase in the percentages of NaCl and sucrose in water. Furthermore, we have measured the sensitivity of the RFID tag at 864, 868, 915, and 926 MHz, respectively, with the same concentrations of the NaCl and Sucrose solutions. The obtained results are presented in Figure 15 and Figure 16, respectively. The obtained results show that for all frequencies the tag sensitivity of the RFID tag increases as the frequency increases. It is found that the best performance of the RFID sensor corresponds to an operating frequency of 864 MHz that ensures the highest sensitivity of the proposed RFID sensor with a change of S_{tag} (6.72/20%) and (9.25/20%) for 864 MHz and 926 MHz, respectively.

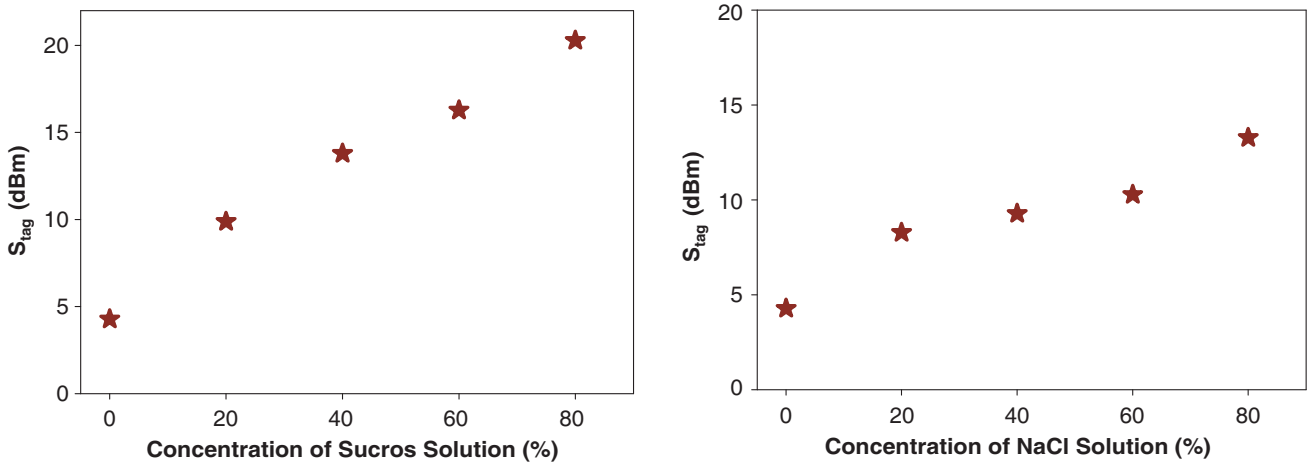

Figure 14. Sensitivity of the RFID tag antenna variation with the different percentage of the Sucrose solution at 915 MHz.

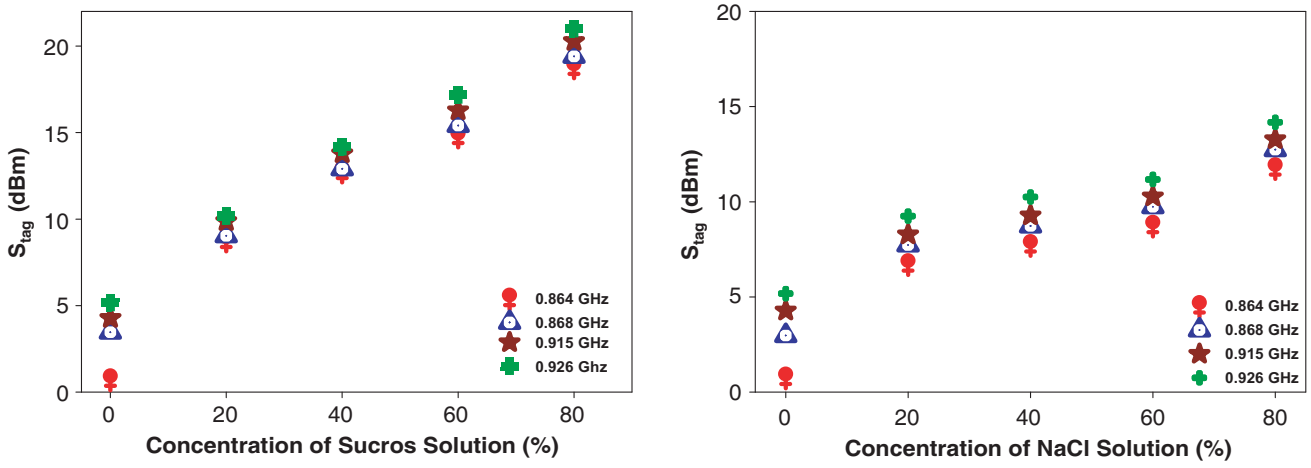

Figure 15. Sensitivity of the RFID tag antenna variation with the different percentage of the NaCl solution as the different frequencies.

The enhancement of the sensitivity of the RFID sensor is about 37%. Hence, the sensor is more likely to detect small concentration variations at the lower bound of the RFID-UHF band.

6. CONCLUSION

In this work, we show the capability of the RFID-UHF technology to detect the concentration of aqueous solutions such as NaCl and sucrose solutions. The proposed low cost flexible RFID tag sensor has a whole size of $100 \times 20\,\mathrm{mm}^2$ and a read range of 5.8 m in free space. The tag sensor sensitivity has been measured and analyzed when there are changes in the concentrations of the NaCl and sucrose in deionized water. The obtained results show that for all frequencies within the RFID-UHF band, the S_{tag} increases with the increment in percentages of NaCl and sucrose concentrations in water. This behavior can be explained by the change in the dielectric constant. Furthermore, the experimental results show that the tag sensitivity is more likely to detect small concentration variations at the lower bound of the RFID-UHF band. The proposed technique has many features such as rapid measurements and lower cost.

REFERENCES

1. Forouzanfar, M. H., L. Alexander, H. R. Anderson, et al., "Global, regional, and national comparative risk assessment of 79 behavioural, environmental and occupational, and metabolic risks or clusters of risks in 188 countries, 1990–2013: A systematic analysis for the Global Burden of Disease Study 2013," *Lancet*, Vol. 386, No. 10010, 323–2287, 2015.
2. Webb, M., S. Fahimi, G. M. Singh, et al., "Cost effectiveness of a government supported policy strategy to decrease sodium intake: Global analysis across 183 nations," *Br. Med. J.*, Vol. 356, i6699, 2017.
3. Johnson, R. J., M. S. Segal, Y. Sautin, T. Nakagawa, D. I. Feig, D.-H. Kang, M. S. Gersch, S. Benner, and L. G. Sánchez-Lozada, "Potential role of sugar (fructose) in the epidemic of hypertension, obesity and the metabolic syndrome, diabetes, kidney disease, and cardiovascular disease," *The American Journal of Clinical Nutrition*, Vol. 86, No. 4, 899–906, Oct. 2007.
4. Islam, M. T., M. N. Rahman, M. S. J. Singh, and M. Samsuzzaman, "Detection of salt and sugar contents in water on the basis of dielectric properties using microstrip antenna-based sensor," *IEEE Access*, Vol. 6, 4118–4126, 2018.
5. Gennarelli, G., S. Romeo, M. R. Scarfi, and F. Soldovieri, "A microwave resonant sensor for concentration measurements of liquid solutions," *IEEE Sensors Journal*, Vol. 13, No. 5, 1857–1864, May 2013.
6. Albishi, A. M. and O. M. Ramahi, "Highly sensitive microwaves sensors for fluid concentration measurements," *IEEE Microwave and Wireless Components Letters*, Vol. 28, No. 4, 287–289, Apr. 2018.
7. Finkenzeller, K., *RFID Handbook: 'Radio-frequency Identification Fundamentals and Applications'*, 2nd Edition, Wiley, New York, NY, USA, 2004.
8. Marrocco, G., L. Mattioni, and C. Calabrese, "Multiport sensor RFIDs for wireless passive sensing of objects — Basic theory and early results," *IEEE Transactions on Antennas and Propagation*, Vol. 56, No. 8, 2691–2702, Aug. 2008.
9. Occhiuzzi, C., C. Paggi, and G. Marrocco, "Passive RFID strain-sensor based on meander-line antennas," *IEEE Transactions on Antennas and Propagation*, Vol. 59, No. 12, 4836–4840, Dec. 2011.
10. Kalansuriya, P., R. Bhattacharyya, and S. Sarma, "RFID tag antenna-based sensing for pervasive surface crack detection," *IEEE Sensors Journal*, Vol. 13, No. 5, 1564–1570, May 2013.
11. Kim, S., Y. Kawahara, A. Georgiadis, A. Collado, and M. M. Tentzeris, "Low-cost inkjet-printed fully passive RFID tags for calibration-free capacitive/haptic sensor applications," *IEEE Sensors Journal*, Vol. 15, No. 6, 3135–3145, Jun. 2015.

12. Wu, X., et al., "Design of a humidity sensor tag for passive wireless applications," *Sensors*, Vol. 15, No. 10, 25564–25576, Basel, Switzerland, Oct. 7, 2015.
13. Caizzone, S., E. Di Giampaolo, and G. Marrocco, "Constrained pole-zero synthesis of phase-oriented RFID sensor antennas," *IEEE Transactions on Antennas and Propagation*, Vol. 64, No. 2, 496–503, Feb. 2016.
14. Escobedo, P., et al., "Passive UHF RFID tag for multispectral assessment," *Sensors*, Vol. 16, No. 7, 1085, Basel, Switzerland, Jul. 14, 2016.
15. Fernández-Salmerón, J., et al., "Passive UHF RFID tag with multiple sensing capabilities," *Sensors*, Vol. 15, No. 10, 26769–26782, Basel, Switzerland, Oct. 22, 2015.
16. Chen, X., L. Ukkonen, and T. Björninen, "Passive E-textile UHF RFID-based wireless strain sensors with integrated references," *IEEE Sensors Journal*, Vol. 16, No. 22, 7835–7836, Nov. 15, 2016.
17. Bhattacharyya, R., C. Floerkemeier, and S. Sarma, "Low-cost, ubiquitous RFID-tag-antenna-based sensing," *Proceedings of the IEEE*, Vol. 98, No. 9, 1593–1600, Sep. 2010.
18. Buchner, R., G. T. Hefter, and P. M. May, "Dielectric relaxation of aqueous NaCl solutions," *J. Phys. Chem. A*, Vol. 103, 1–9, 1999.
19. Malmberg, C. G. and A. A. Maryott, "Dielectric constants of aqueous solutions of dextrose and sucrose," *Journal of Research of the National Bureau of Standards*, Vol. 45, No. 4, Oct. 1950.
20. http://www.murata.com/∼/media/webrenewal/support/library/catalog/products/k70e.ashx.
21. Daiki, M., H. Chaabane, E. Perret, S. Tedjni, and T. Aguili, "RFID chip impedance measurement for UHF tag design," *PIERS 2011 in Marrakesh Proceedings*, 679, Marrakesh, Morocco, Mar. 20–23, 2011.
22. Miron, D. B., *Small Antenna Design*, Newnes, Burlington, MA, USA, 2006.
23. Terman, F. E., *Radio Engineer's Handbook*, McGraw-Hill, New York, 1945.
24. http://www.triumphlaser.com/laser-cutting-system/.
25. Qing, X., C. K. Goh, and Z. N. Chen, "Impedance characterization of RFID tag antennas and application in tag co design," *IEEE Transactions on Microwave Theory and Techniques*, Vol. 57, No. 5, 1268–1274, May 2009.
26. Kraus, J. D. and R. J. Marhefka, *Antennas*, 3rd edition, Chapter 13, McGraw-Hill, 2002.
27. Deleruyelle, T., P. Pannier, M. Egels, and E. Bergeret, "Dual band mono-chip HF-UHF tag antenna," *Proc. IEEE Antennas Propag. Soc. Int. Symp.*, 1–4, Toronto, Canada, Jul. 2010.
28. Colella, R., L. Catarinucci, P. Coppola, and L. Tarricone, "Measurement platform for electromagnetic characterization and performance evaluation of UHF RFID tags," *IEEE Transactions on Instrumentation and Measurement*, Vol. 65, No. 4, 905–914, Apr. 2016.